



# Full model-based iterative reconstruction (MBIR) in abdominal CT increases objective image quality, but decreases subjective acceptance

Gautier Laurent<sup>1</sup> · Nicolas Villani<sup>2</sup> · Gabriela Hossu<sup>3</sup> · Aymeric Rauch<sup>1</sup> · Alain Noël<sup>4</sup> · Alain Blum<sup>1</sup> · Pedro Augusto Gondim Teixeira<sup>1</sup>

Received: 27 August 2018 / Revised: 25 November 2018 / Accepted: 19 December 2018 / Published online: 30 January 2019  
© European Society of Radiology 2019

## Abstract

**Objective** Evaluate and compare the image quality and acceptance of a full MBIR algorithm to that of an earlier full IR hybrid algorithm and filtered back projection (FBP).

**Methods** Acquisitions were performed with a 320 detector-row CT scanner with seven different dose levels. Images were reconstructed with three algorithms: FBP, full hybrid iterative reconstruction (HIR), and a full model-based iterative reconstruction algorithm (full MBIR). The sensitometry, spatial resolution, image texture, and low-contrast detectability of these algorithms were compared. Subjective analysis of low-contrast detectability was performed. Ten radiologists answered a questionnaire on image quality and confidence in full MBIR images in clinical practice.

**Results** The contrast-to-noise ratio of full MBIR was significantly higher than in the other algorithms ( $p < 0.0015$ ). The spatial resolution was also higher with full MBIR at high frequencies ( $> 0.3$  lp/mm). Full MBIR at low dose levels led to better low-contrast detectability and more inserts being identified with a higher confidence ( $p < 0.0001$ ). Full MBIR was associated with a change in image texture compared to HIR and FBP. Eighty percent of radiologists judged general appearance and texture of full MBIR images worse than HIR. Moreover, compared with HIR, for 50% of radiologists, the diagnostic confidence on full MBIR images was worse. Questionnaire reliability was considered acceptable (Cronbach alpha 0.7).

**Conclusion** Compared to conventional iterative reconstruction algorithms, full MBIR presented a higher image quality and low-contrast detectability and a worse acceptance among radiologists.

## Key Points

- Full MBIR used led to an overall improvement in image quality compared with FBP and HIR.
- Full MBIR leads to image texture change which reduces the confidence in these images among radiologists.
- Awareness of the image texture change and improved quality of full MBIR reconstructed images could improve the acceptance of this technique in clinical practice.

**Keywords** Computed tomography · Image reconstruction · Image quality · Phantom imaging · Abdomen

## Abbreviations

AIDR	Adaptative statistical iterative reconstruction
CNR	Contrast-to-noise-ratio
CT	Computed tomography
CTP	Catphan phantom
FBP	Filtered back projection
HIR	Hybrid iterative reconstruction
HU	Hounsfield units
IR	Iterative reconstruction
LDPE	Low density polyethylene
MBIR	Model-based iterative reconstruction
MTF	Modulation transfer function
NPS	Noise power spectrum
ROI	Region of interest

✉ Gautier Laurent  
gautierlaurent54@gmail.com

<sup>1</sup> Guilloz Imaging Department, Central Hospital, University Hospital Center of Nancy, 29 Avenue du Maréchal de Lattre de Tassigny, 54035 Nancy Cedex, France

<sup>2</sup> Medical Radiophysical Unit, Centre Alexis-Vautrin, 6 Avenue de Bourgogne, 54129 Vandoeuvre-lès-Nancy, France

<sup>3</sup> Université de Lorraine, Inserm, IADI, F-54000 Nancy, France

<sup>4</sup> CRAN UMR 7039 Université de Lorraine-CNRS, Villers-lès-Nancy, France

## Introduction

CT is responsible for a significant portion of health care-related patient exposure to ionizing radiation with potential impact on the development of secondary neoplasm [1]. Iterative reconstruction (IR) algorithms play an important role in dose reduction allowing for the same image quality with reductions of more than half of the patient delivered dose [2–4]. The first generations of IR algorithms were based on series of independent comparisons (iterations) between a single model (filtered back projection—FBP reconstructed image) and actual data. This iterative process can be done in the image domain alone or in both image and raw data domains (full iterative reconstruction) [5]. Recently, a new generation of IR algorithms became available. It uses image reconstruction with an iterative correction process that considers multiple models that account for scanner hardware parameters, cone beam trajectory, photoelectric trajectory, etc. These algorithms can also be active in both image and raw data domains (full model-based iterative reconstruction—full MBIR) maintaining image quality at lower dose levels while increasing image resolution [6–12].

The clinical use of full MBIR is, however, not without difficulty. MBIR leads to considerable changes in image texture compared to earlier IR algorithms with images appearing coarser and plastic-like (Fig. 1). These image texture changes are related to the magnitude of image quantum noise which is also dependent on multiple factors (dose, patient body habitus, reconstruction kernel, etc.). Compared to FBP, IR algorithms change the quantum noise frequency distribution on the images. IR algorithms and full MBIR in particular lead to a signal change from higher frequencies to lower frequencies, which translates visually to a coarser image granulation [13]. These changes may lead to acceptance problems among radiologists who tend to be less confident when interpreting full MBIR images. These algorithms are also time consuming as it requires more computational power compared to non-MBIR techniques. Specific hardware is sometimes required to keep reconstruction time within

acceptable range and an abdomino pelvic CT study can still take 5 to 15 min of reconstruction time depending on the vendor [14].

In this study, the performance of a full MBIR algorithm already available for clinical use in the field of abdominal imaging was assessed. First, a phantom study was performed to compare the performance of this algorithm to that of an earlier full IR hybrid algorithm and FBP. Then, algorithm performance for low-contrast detection, which is a meaningful parameter for the evaluation of IR algorithms with different dose levels [15], as well as the acceptance level of generated images were evaluated subjectively by a group of university hospital radiologists and residents from specialties other than radiology with no prior knowledge of the expected appearance of CT images. This information may help ascertain the role of full MBIR in clinical practice and may help improve the confidence of radiologists working with this type of images.

## Material and methods

### Phantom acquisitions

All acquisitions were performed with a 320 detector-row CT scanner (Aquilion ONE, Canon Medical Systems) with seven different dose levels (Table 1). All acquisitions shared the following parameters: matrix  $512 \times 512$ , field-of-view  $220 \times 220$  mm, 120 kV, 35 to 250 mA, slice thickness 0.5 mm, z-axis coverage 40 mm, and a 1-s tube rotating speed. All images were reconstructed using a soft tissue kernel and a slice thickness of 1 mm.

### Reconstruction algorithms

All images were reconstructed with three algorithms: FBP, HIR (full hybrid iterative reconstruction) (AIDR 3D—adaptive statistical iterative reconstruction, Canon Medical Systems) and full MBIR (FIRST—forward projected model-

**Fig. 1** Low-dose abdominal (kV = 120, mAs = 90) CT in the portal phase from a 20-year-old female reconstructed with HIR (a) and full MBIR (b) algorithms. Note that noise level is lower on full MBIR image compared to HIR and presents a different image texture with a more plastic-like appearance

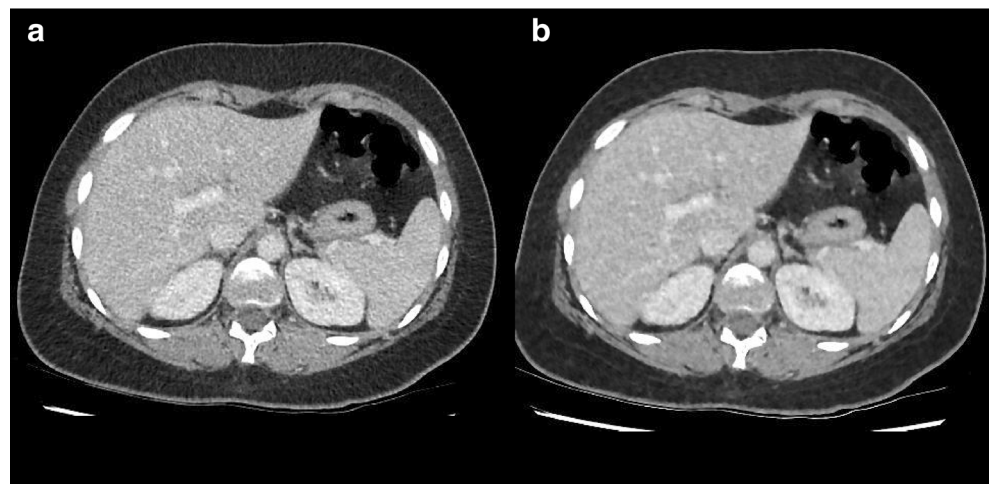


**Table 1** Protocol settings for the seven dose levels evaluated

mA	CTDI (vol)	DLP (mGy × cm)
35	2.9	61.2
50	4.2	87.5
70	5.9	122.4
100	8.4	174.9
120	10.1	209.9
150	12.6	262.4
250	21	437.3

based iterative reconstruction—body, Canon Medical Systems). HIR adaptively performs noise reduction according to the actual scanning conditions and to the statistics of electronic and quantum noise. It then applies an iterative algorithm of data improvement in the image domain and adapts to different organs and reconstruction filters. Full MBIR optimizes the image quality in the raw data domain with a direct projection model which takes into account system geometry, optical system, cone angle, and a statistical modelization of noise in density measurements. It also provides an independent noise penalty function which compares the initial image to the original projection data to identify the differences in Hounsfield units (HU) in adjacent pixels so as to retrace the noise level in the images. For both HIR and full MBIR algorithms, a medium iteration level was used; it was the standard manufacturer recommendation. The soft tissue kernel used for FBP and HIR (FC08) is not exactly the same one used for full MBIR since with the latter algorithm the reconstruction kernel is integrated in the iterative process. The FC08 soft tissue kernel was chosen because the manufacturer indicated it was the kernel most similar to that of full MBIR.

## Phantom study

Phantom images were analyzed with two software programs: ImageJ 1.48v (National Institute of Health) and IQworks V0.7.2 (<http://iqworks.org/>). The following modules of a CATPHAN 600, 6th generation (The Phantom Laboratory, Incorporated) were used:

**CTP404 module** It includes four peripheral inserts made of Teflon, polystyrene, LDPE (low density polyethylene), and air, with different contrast attenuation (6.243, 3.335, 3.16, and  $0.004 \text{ e/cm}^3 \times 10^{23}$  respectively). These contrast attenuation value range correspond to HU references provided with the phantom (air:  $-1046$ – $-986$  HU; LDPE:  $-121$ – $-87$  HU; polystyrene:  $-65$ – $-29$  HU; Teflon:  $941$ – $1060$  HU). A measurement error was considered moderate when absolute values differed from reference standards in more than 5% and substantial when they differed more than 10%. This module was also used to evaluate the contrast-to-noise ratio (CNR) which was calculated as follows:

$$\text{CNR} = (\text{mean insert density} - \text{mean background density}) / \text{standard deviation of the background density}$$

This module also includes five central acrylic inserts of 2, 4, 6, 8, and 10 mm, which were used for subjective low-contrast detection (Fig. 2). For this purpose, 10 residents of specialties other than radiology with no previous knowledge of reconstruction algorithm-related image changes and 10 senior radiologists confronted to FBP, HIR, and full MBIR reconstructed images in their daily practice evaluated the central image of 12 acquisitions (three reconstruction algorithms with four dose levels each). Phantom images were displayed in random positions to avoid memorization bias during readouts. All images were displayed in real size with identical window settings (width and level of 400 and 40 HU). Readers were blinded for reconstruction algorithm and dose level used. The number of inserts detected and confidence in detection were assessed. The detection confidence was graded as follows:

- 1) Barely distinguishable insert, the reader not certain of its existence
- 2) Insert is partially seen, the reader is confident in its existence
- 3) Insert unequivocally present

Identification errors were taken into account. The global subjective analysis score varied from 0 to 2. It was composed of the ratio of correctly detected inserts (*number of detected*

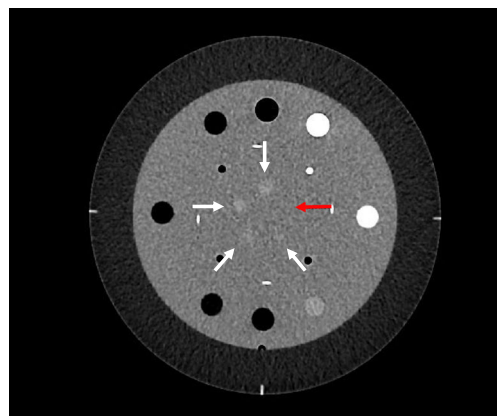


**Fig. 2** Axial CT image of the phantom's CTP 404 module. The five central acrylic inserts of 10, 8, 6, 4, and 2 mm which the location is indicated by the arrows. The 2 mm insert cannot be distinguished in this image red arrow. These inserts were used for subjective low-contrast detection. Acquisitions with three dose levels with images reconstructed with the three reconstruction algorithms studied were evaluated for the number of inserts detected and confidence in detection by each reader

*inserts/total number of inserts*) added to the confidence grade ratio of the correctly identified inserts (*number of detected inserts* × *confidence grade/maximum confidence*). Maximum confidence was calculated by multiplying the number of correctly detected inserts (from 0 to 5) by the confidence grade of each correctly identified insert (1 to 3) and thus varied from 0 to 15.

**CTP 515 module** It contains 27 peripheral cylindrical inserts (insert groups of nine different diameters with three density levels each—1%, 0.5%, and 0.3%), which were used for objective low-contrast detectability. All inserts and the surrounding material have equal atomic numbers with concentration differences accounting for density variation. For this purpose, a region-of-interest (ROI) was positioned at the center of 12 of the largest inserts to avoid ROI positioning errors. Five, four, and three inserts were evaluated in each density level group (from high to low density level groups). The diameters of the evaluated inserts were 15 mm, 9 mm, 8 mm, 7 mm, and 6 mm. In addition, three ROIs were positioned in the background. Contrast-to-noise ratio (CNR) was calculated as previously described. The threshold of detection level was arbitrarily defined as a CNR of 0.9. If the CNR was higher than 0.9, the region was considered detectable, and if it was lower than 0.9 the insert was considered undetectable.

**CTP528 module** This module contains a high resolution test gauge (from 1 to 21 line pairs per centimeter) for spatial resolution evaluation. It also has a bead point source for point spread function and modulation transfer function (MTF) assessment.

**CTP 486 module** Composed of a uniform material yielding a density close to water in HU, this module was used for the calculation of the NPS.

### Assessment of full MBIR in clinical practice

A questionnaire was submitted to 10 radiologists who have been working for at least a year with abdominal images reconstructed with both HIR and full MBIR. The questionnaire aims at comparing the overall appearance, texture, noise level and diagnostic confidence using full MBIR imaging with respect to HIR, which has been used in our institution for over 6 years and was used as the standard of reference. A 5-point Likert scale varying from “much better” to “much worse” was used (Fig. 3).

### Statistical analysis

Statistical analysis was performed with the R Development Core Team software (version 3.0.12013). Statistical significance of CNR variation, the number of inserts detected

Clinical practice assessment questionnaire
1. How do you judge full MBIR image appearance compared to images reconstructed with HIR in your clinical routine practice?
2. How do you judge full MBIR image texture compared to HIR?
3. How do you judge full MBIR image noise level compared to HIR?
4. How do you judge full MBIR image diagnostic confidence level compared to HIR?

**Fig. 3** Questionnaire used for the clinical practice assessment of full MBIR. Evaluators were asked to answer with the following Likert scale: much worse, slightly worse, similar, slightly better, and much better

subjectively and the confidence in detection with the different reconstruction algorithms were compared with the Wilcoxon rank test. The Holm  $p$  value correction method was used to counteract the problem of multiple comparisons. Linear regression analysis was used to evaluate the influence of the reconstruction algorithm and medical specialty on the number of targets detected subjectively. Questionnaire response reliability was estimated by calculating the Cronbach alpha coefficient ( $\alpha$ ). Reliability was considered excellent if  $\alpha$  was higher than 0.9; good if it was between 0.9 and 0.8; acceptable if it was between 0.8 and 0.7; questionable if it was between 0.7 and 0.6; poor if it was between 0.6 and 0.5, and unacceptable if it was under 0.5. A  $p$  value of 0.05 was used as the threshold of statistical significance.

## Results

### Sensitometry

As expected, the greatest estimation errors were found with inserts in the extremes of the densities evaluated (air and Teflon) (Table 2). With both IR algorithms, there were no estimation errors on inserts with intermediate densities (polystyrene and LDPE). With full MBIR, the mean error was moderate for air and Teflon regardless of the acquisition dose level. HIR showed substantial density estimation for Teflon in all dose levels. With FBP in addition to inserts in the extremes of density, there were errors with intermediate density LDPE inserts with 35 and 250 mA acquisitions.

CNR was influenced by acquisition dose regardless of the reconstruction algorithm. CNR improved as acquisition dose was increased in materials of all densities. Compared to FBP and HIR, the CNR of full MBIR was significantly higher in all materials and dose levels evaluated ( $p < 0.0015$ ). These differences were particularly important in materials in the extremes of density. For instance, with a 250 mA acquisition on air, CNR was 78% and 150% higher for full MBIR with respect

**Table 2** Sensitometry error evaluation with FBP, HIR, and full MBIR

Material	Expected density	35 mA		100 mA		250 mA	
		Measured	Error	Measured	Error	Measured	Error
Full MBIR							
Air	-1046:-986	-963.5	> 5%	-965.8	> 5%	-969.9	> 5%
LDPE	-121:-87	-89.1	< 5%	-90.3	< 5%	-89.4	< 5%
Polystyrene	-65:-29	-33.5	< 5%	-32.4	< 5%	-35.1	< 5%
Teflon	941:1060	933.0	> 5%	937.5	> 5%	939.5	> 5%
HIR							
Air	-1046:-986	-965.1	> 5%	-973.6	> 5%	-972.3	> 5%
LDPE	-121:-87	-87.2	< 5%	-88.8	< 5%	-87.8	< 5%
Polystyrene	-65:-29	-34.1	< 5%	-33.6	< 5%	-34.4	< 5%
Teflon	941:1060	861.1	> 10%	865.8	> 10%	863.3	> 10%
FBP							
Air	-1046:-986	-957.2	> 5%	-962.8	> 5%	-965.1	> 5%
LDPE	-121:-87	-86.3	> 5%	-88.0	< 5%	-86.9	> 5%
Polystyrene	-65:-29	-33.1	< 5%	-33.3	< 5%	-33.8	< 5%
Teflon	941:1060	856.4	> 10%	858.9	> 10%	857.0	> 10%

LDPE low density polyethylene

to HIR and FBP respectively. For Teflon, these figures were 94% and 214% (Fig. 4).

## Spatial resolution

MTF analysis showed that for all dose levels, full MBIR spatial resolution is higher for 10% and 50% MTF levels (between the frequencies of 0.4 and 0.8 lp/mm) with respect to HIR and FBP. There was a gain in spatial resolution from FBP to HIR for 10 and 50% MTF levels; however, the spatial resolution of both these algorithms remained considerably lower than that of full MBIR (Fig. 5). Visually, these spatial resolution differences were only perceptible when full MBIR

was compared with HIR and FBP but not when HIR and FBP were compared among themselves (Fig. 6).

## Image texture

NPS analysis showed a shorter frequency distribution of signal with full MBIR, whatever the dose, with curve center on lower frequencies. With FBP and HIR, the frequency bandwidth was higher and curves were centered on higher frequencies compared to full MBIR, which translates to a coarser image texture for the latter algorithm. Image texture with Full MBIR was also influenced by acquisition dose. Regardless of the algorithm, decreasing the acquisition dose

**Fig. 4** CNR measurements in four materials of different density at three doses levels of 35 mA, 100 mA, and 250 mA reconstructed with full MBIR, HIR, and FBP. Note that the CNR of full MBIR is higher in all materials and all dose levels evaluated

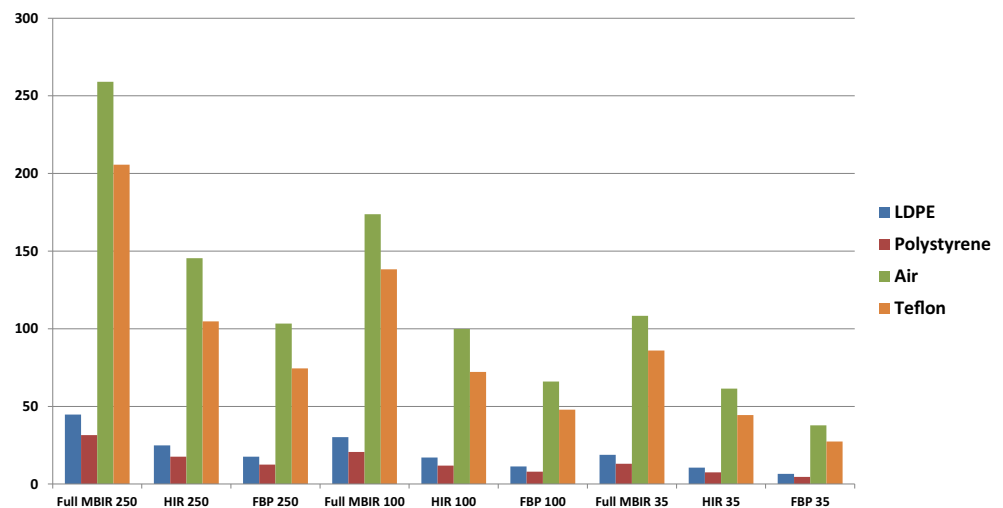
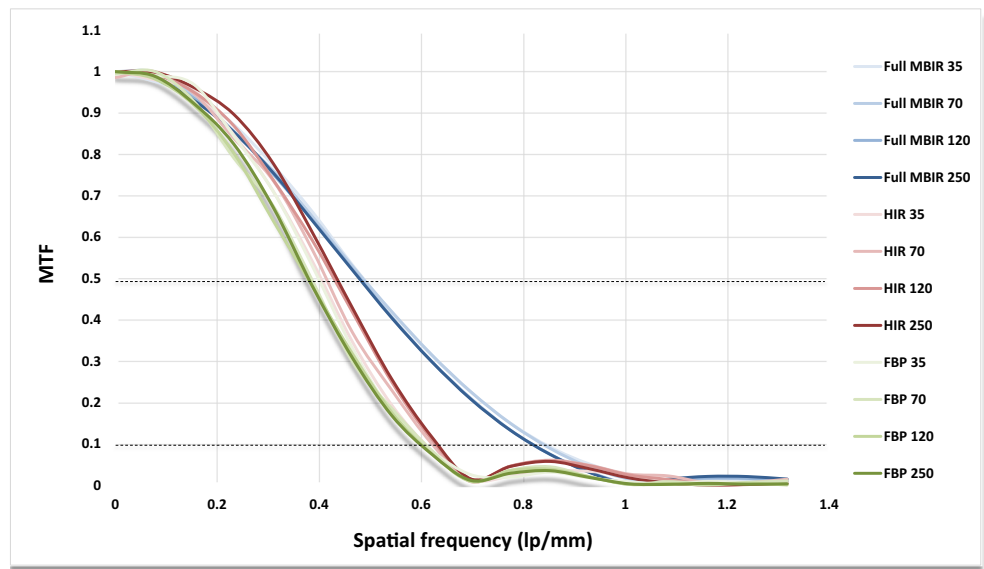


**Fig. 5** MTF curves for full MBIR, HIR, and FBP with four different dose levels. Note that Full MBIR (blue curves) spatial resolution is higher for 10% and 50% MTF levels (between the frequencies of 0.4 and 0.8 lp/mm) with respect to HIR and FBP (red and green curves) in all dose levels



led to an increase in the amplitude of the noise without modifying the peak nor the general aspect of the spectrum. As there is more noise at lower frequencies, this results in increased image texture coarseness (Fig. 7).

**Low-contrast detectability**

**Objective analysis**

At all dose levels, full MBIR performed better than HIR, with mean CNR values of  $1.29 \pm 0.4$  versus  $0.72 \pm 0.17$

respectively. This translated into a median of  $7 \pm 1.63$  inserts detected with full MBIR and  $4 \pm 0.95$  with HIR. The performance of FBP (mean CNR of  $0.48 \pm 0.14$  and median of detected inserts of  $2 \pm 1.35$ ) was slightly lower than that of HIR (Table 3).

**Subjective analysis**

Full MBIR performed better than FBP and HIR at all dose levels for the number of detected inserts ( $p < 0.0001$ ) and global score ( $p < 0.0001$ ) (Fig. 8). This difference

**Fig. 6** Axial CT image demonstrating the visual aspect of the CTP528 module at the lower dose level (35 mA) with the three reconstruction algorithms evaluated with a window level of 300 HU and a width of 2500 HU. Note the clearer aspect of the phantom gauges with full MBIR (C) compared to FBP and HIR. This effect is particularly well seen at the 7 and 8 line pairs (lp) gauges (arrows). Note also that there is no perceptible change in spatial resolution from FBP to HIR; however, with full MBIR, a perceptible improvement in spatial resolution is seen

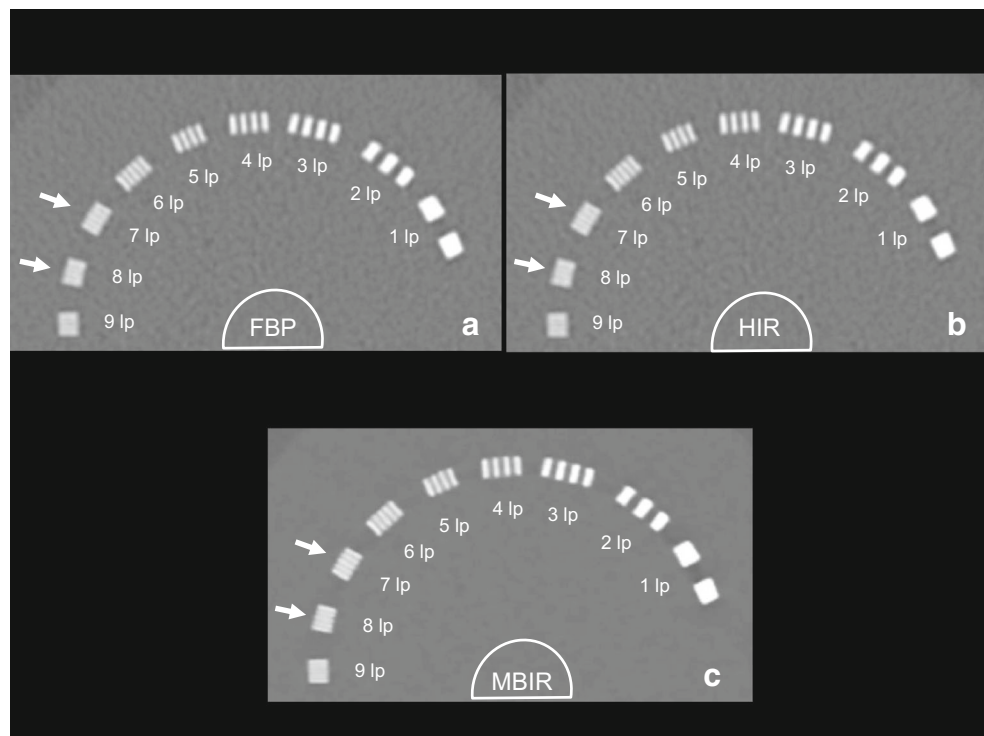
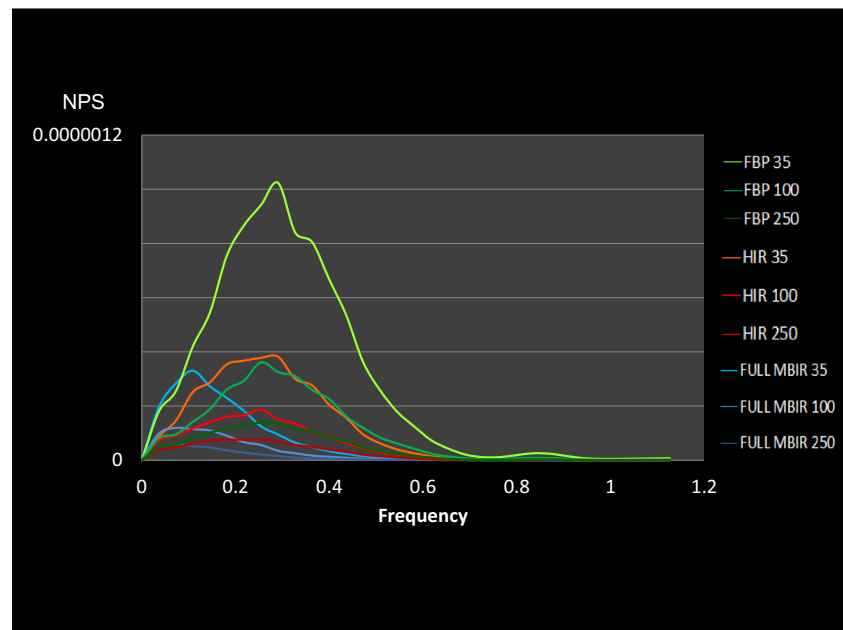


**Fig. 7** NPS (noise power spectrum) curves with full MBIR (blue tone curves), HIR (red tone curves), and FBP (green tone curves) at three different dose levels of 250 mA, 100 mA, and 35 mA. Note that regardless of the dose with full MBIR signal (blue) is concentrated in a lower bandwidth, which translates into images with a coarser texture (not shown)



increased as the dose was lowered and was greatest at the lowest dose (35 mA) with a mean number of detected inserts of  $2.85 \pm 0.85$  targets (out of five) with a global score of  $0.94 \pm 0.35$  with full MBIR compared to  $1.35 \pm 1.19$  inserts detected with a global score of  $0.4 \pm 0.37$  for HIR and  $1.3 \pm 1.23$  inserts detected with a global score of  $0.37 \pm 0.35$  for FBP. The mean number of detected inserts and global scores of the three algorithms evaluated are presented in Table 4. It should be noted that non-radiologists detected more inserts than radiologists (mean number of detected inserts of  $3.5 \pm 0.6$  and  $3.2 \pm 0.9$  respectively), with

a similar trend towards higher detection rates with full MBIR ( $p = 0.0024$ ).

### Subjective image quality appreciation

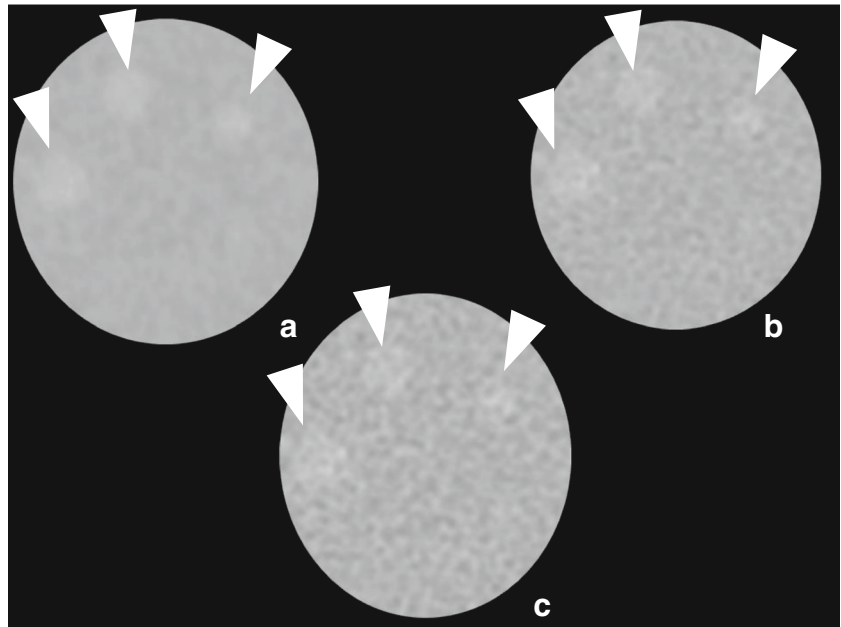
Answer reliability was considered acceptable with a Cronbach alpha value of 0.7. Seven out of 10 radiologists surveyed judged the general appearance of full MBIR images slightly worse than HIR and one radiologist graded it as much worse (mean score  $2.1 \pm 0.5$ ). Image texture with full MBIR was also considered slightly worse by six radiologists and much worse

**Table 3** Objective evaluation of low-contrast detectability of 12 cylindrical inserts of four different diameters and three density levels each with the three algorithms

CNR threshold = 0.9 Acquisition protocol	Full MBIR			HIR			FBP		
	CNR mean	CNR Sdev	Identified inserts	CNR mean	CNR Sdev	Identified inserts	CNR mean	CNR Sdev	Identified inserts
250 mA	1.91	1.31	9	0.98	0.68	5	0.68	0.52	4
150 mA	1.66	0.95	9	0.84	0.52	4	0.59	0.41	4
120 mA	1.21	0.78	7	0.67	0.47	3	0.41	0.34	2
100 mA	1.15	0.75	7	0.58	0.41	4	0.42	0.31	1
70 mA	1.40	0.88	7	0.81	0.65	4	0.57	0.44	2
50 mA	0.88	0.61	5	0.72	0.35	4	0.43	0.33	1
35 mA	0.80	0.47	5	0.46	0.39	2	0.25	0.32	1
Mean	1.29	0.82	7.00	0.72	0.50	4.00	0.48	0.38	2.00
SD	0.40	0.27	1.63	0.17	0.13	0.95	0.14	0.08	1.35

CNR contrast to noise ratio, SD standard deviation, MBIR model-based iterative reconstruction, HIR hybrid iterative reconstruction, FBP filtered back projection

**Fig. 8** CT images of the central portion of the phantom’s CTP 404 module reconstructed with Full MBIR (a), HIR (b), and FBP (c). Images were acquired with the 250 mA acquisition protocol. The three largest inserts are identified in each image by the white arrowheads. Note the differences in noise, increasing from full MBIR to HIR to FBP and image texture which appears coarser in full MBIR images compared to HIR and FBP. Note also the increase in conspicuity of the inserts in full MBIR compared to HIR and FBP



by two (mean score  $2.1 \pm 0.8$ ). Conversely, image noise level with full MBIR was considered similar or slightly better by seven out of 10 radiologists (mean score  $2.8 \pm 1.1$ ). Finally, diagnostic confidence level with full MBIR was considered worse than HIR by five out of ten radiologists and identical by four (mean score  $2.2 \pm 0.7$ ). Only one radiologist considered diagnostic confidence to be slightly better with full MBIR.

**Discussion**

The application of full MBIR yielded paradoxical results. Compared to FBP and HIR, there was an overall improvement in image quality with full MBIR with a concomitant decrease in the acceptance of full MBIR images by radiologists. The sensitivity, spatial resolution, and CNR were improved with full MBIR compared to the other tested algorithms and these differences were higher at low dose levels which could translate into a

better performance in clinical practice. Objective assessment of low-contrast detectability shows a superiority of full MBIR in insert detection compared to HIR in all dose levels. Similarly, subjective low-contrast detectability was better than HIR with a significantly higher detection rate and global scores for both radiologists and non-radiologists ( $p < 0.0001$ ). These results match previous literature reports and support the clinical use of full MBIR, which also provides the highest potential to cope with low dose protocols [2, 3, 16, 17].

Full MBIR is associated with changes in image texture related to the fact that signal is distributed within a narrow bandwidth of frequencies compared to HIR and FBP, which accounts for a coarser image texture. We believe that this texture change might influence the radiologist’s confidence for image interpretation. Eighty percent of the participating radiologists judged general quality of full MBIR images worse than HIR, half judged the image texture worse and 50% indicated lower confidence in diagnosis when using full MBIR.

**Table 4** Subjective analysis results for radiologists and non-radiologists. Up to five inserts could be identified and global scores ranged from 0 to 15

	Detected inserts	Global score						
	Full MBIR 35		Full MBIR 70		Full MBIR 120		Full MBIR 250	
Mean	2.85	0.94	3.4	1.17	3.65	1.25	3.6	1.35
SD	0.85	0.35	0.91	0.36	0.65	0.29	0.49	0.21
	HIR 35		HIR 70		HIR 120		HIR 250	
Mean	1.35	0.4	2.85	1.01	2.9	1.02	3.15	1.17
SD	1.19	0.37	0.48	0.17	0.77	0.31	0.48	0.19
	FBP 35		FBP 70		FBP 120		FBP 250	
Mean	1.3	0.37	1.35	0.41	2.7	0.91	2.7	0.93
SD	1.23	0.35	1.19	0.39	0.71	0.27	0.71	0.29

SD standard deviation, *Insert* number of identified inserts

These results contrast with the higher performance of full MBIR in terms of spatial resolution and low-contrast detectability found in the phantom study. Moreover, non-radiologists with no familiarity with CT images detected more low-contrast inserts than radiologists. It is likely that the change in image texture generated by full MBIR, which translates to a plastic image appearance, has a negative effect on the appreciation of full MBIR images for readers used to conventional IR algorithms. In the studied population, this effect seemed to overcome the potential diagnostic benefits of full MBIR as in their clinical practice there was a clear preference towards HIR among the radiologists. This information has important potential implications since the increased awareness of the potential benefits of full MBIR for abdominal imaging despite the change in texture could help improve the acceptance of this algorithm in clinical practice. Moreover, this information should be taken in consideration during the training programs of future radiologists.

Our results differ from those presented by Euler et al who did not show any difference between MBIR and FBP reconstructed images for low-contrast detection on abdominal CT scans in a subjective analysis by 12 radiologists [18]. This discordance might be explained by differences in the MBIR algorithm used in the insert sizes evaluated, which were of smaller size in the present study. Our results are, however, in accordance with two other studies. Solomon et al showed better performance of MBIR versus FBP for low-contrast detection with low dose acquisitions and Gordic et al who also reported a better performance of a MBIR algorithm for pulmonary nodules detection [19]. In many of the previous studies however, MBIR algorithms are compared to FBP and not to conventional IR algorithms which can be considered as standard in today's radiologic practice [20].

This study has some limitations that need to be acknowledged. Firstly, a single MBIR algorithm and one type of CT scanner model were evaluated. Although the basic principles between MBIR algorithms are similar, different algorithms and different scanner models might have a variable impact on image quality and texture. Secondly, this was a phantom study and it is important to keep in mind that image quality improvements reported with full MBIR, including low-contrast detectability, do not necessarily translate to a higher diagnostic accuracy. The actual diagnostic impact of full MBIR in clinical practice should be validated by further patient studies. Moreover, other factors affecting CT image quality on CT such as matrix size, FOV, patient body habitus, and the presence of metal implants were not evaluated in this study. These results cannot be directly transposed to CT imaging of other body regions such as lungs, cardiac, or bone, which may require specific MBIR algorithms.

In conclusion, the evaluated full MBIR algorithm has the potential to improve image quality and contribute to patient dose reduction in abdominal CT studies, with more reliable

densitometry, higher spatial resolution for higher frequencies, and better low-contrast detectability, particularly in lower dose protocols. Although the radiologist's acceptance of full MBIR images was worse, the phantom diagnostic performance was better with respect to conventional IR and FBP. Full MBIR considerably alters image texture which may reduce confidence in the reconstructed images and therefore have a potential impact on diagnostic performance.

**Funding** The authors state that this work has not received any funding.

## Compliance with ethical standards

**Guarantor** The scientific guarantor of this publication is Professor Pedro Augusto Gondim Teixeira.

**Conflict of interest** Two authors involved in this work (Pedro Augusto Gondim Teixeira and Alain Blum) participate on a non-remunerated research contract with CANON medical Systems for the development and clinical testing of post processing tools for CT. The others authors have non-potential conflicts of interest to disclose.

**Statistics and biometry** One of the authors, Gabriela Hossu, PhD, is a statistician.

**Ethical approval** Institutional Review Board approval was not required because this was a phantom based study.

## Methodology

- prospective
- experimental
- performed at one institution

**Publisher's note** Springer Nature remains neutral with regard to jurisdictional claims in published maps and institutional affiliations.

## References

1. Parplys AC, Petermann E, Petersen C, Dikomey E, Borgmann K (2012) DNA damage by X-rays and their impact on replication processes. *Radiother Oncol* 102:466–471
2. Ellmann S, Kammerer F, Allmendinger T et al (2018) Advanced modeled iterative reconstruction (ADMIRE) facilitates radiation dose reduction in abdominal CT. *Acad Radiol* 25(10):1277–1284
3. Mello-Amoedo CD, Martins AN, Tachibana A, Pinho DF, Baroni RH (2018) Comparison of radiation dose and image quality of abdominopelvic CT using iterative (AIDR 3D) and conventional reconstructions. *AJR Am J Roentgenol* 210:127–133
4. Zinsser D, Marcus R, Othman AE et al (2018) Dose reduction and dose management in computed tomography - state of the art. *Rofo* 190:531–541
5. Willemink MJ, de Jong PA, Leiner T et al (2013) Iterative reconstruction techniques for computed tomography part 1: technical principles. *Eur Radiol* 23:1623–1631
6. Chang W, Lee JM, Lee K et al (2013) Assessment of a model-based, iterative reconstruction algorithm (MBIR) regarding image quality and dose reduction in liver computed tomography. *Invest Radiol* 48:598–606
7. Husarik DB, Alkadhi H, Puipe GD et al (2015) Model-based iterative reconstruction for improvement of low-contrast

- detectability in liver CT at reduced radiation dose: ex-vivo experience. *Clin Radiol* 70:366–372
8. Ohno Y, Yaguchi A, Okazaki T et al (2016) Comparative evaluation of newly developed model-based and commercially available hybrid-type iterative reconstruction methods and filter back projection method in terms of accuracy of computer-aided volumetry (CADv) for low-dose CT protocols in phantom study. *Eur J Radiol* 85:1375–1382
  9. Vardhanabhuti V, Riordan RD, Mitchell GR, Hyde C, Roobottom CA (2014) Image comparative assessment using iterative reconstructions: clinical comparison of low-dose abdominal/pelvic computed tomography between adaptive statistical, model-based iterative reconstructions and traditional filtered back projection in 65 patients. *Invest Radiol* 49:209–216
  10. Volders D, Bols A, Haspeslagh M, Coenegrachts K (2013) Model-based iterative reconstruction and adaptive statistical iterative reconstruction techniques in abdominal CT: comparison of image quality in the detection of colorectal liver metastases. *Radiology* 269:469–474
  11. Yamada Y, Jinzaki M, Tanami Y et al (2012) Model-based iterative reconstruction technique for ultralow-dose computed tomography of the lung: a pilot study. *Invest Radiol* 47:482–489
  12. Yasaka K, Katsura M, Akahane M, Sato J, Matsuda I, Ohtomo K (2016) Model-based iterative reconstruction and adaptive statistical iterative reconstruction: dose-reduced CT for detecting pancreatic calcification. *Acta Radiol Open* 5:2058460116628340
  13. Khobragade P, Fan J, Rupcich F, Crotty DJ, Schmidt TG (2018) Application of fractal dimension for quantifying noise texture in computed tomography images. *Med Phys*. <https://doi.org/10.1002/mp.13040>
  14. Geyer LL, Schoepf UJ, Meinel FG et al (2015) State of the art: iterative CT reconstruction techniques. *Radiology* 276:339–357
  15. Schindera ST, Odedra D, Raza SA et al (2013) Iterative reconstruction algorithm for CT: can radiation dose be decreased while low-contrast detectability is preserved? *Radiology* 269:511–518
  16. McCollough CH, Bartley AC, Carter RE et al (2017) Low-dose CT for the detection and classification of metastatic liver lesions: results of the 2016 low dose CT grand challenge. *Med Phys* 44:e339–e352
  17. Tang H, Yu N, Jia Y et al (2018) Assessment of noise reduction potential and image quality improvement of a new generation adaptive statistical iterative reconstruction (ASIR-V) in chest CT. *Br J Radiol* 91:20170521
  18. Euler A, Stieltjes B, Szucs-Farkas Z et al (2017) Impact of model-based iterative reconstruction on low-contrast lesion detection and image quality in abdominal CT: a 12-reader-based comparative phantom study with filtered back projection at different tube voltages. *Eur Radiol* 27:5252–5259
  19. Gordic S, Morsbach F, Schmidt B et al (2014) Ultralow-dose chest computed tomography for pulmonary nodule detection: first performance evaluation of single energy scanning with spectral shaping. *Invest Radiol* 49:465–473
  20. Kataria B, Althén JN, Smedby Ö, Persson A4, Sökjer H, Sandborg M (2018) Assessment of image quality in abdominal CT: potential dose reduction with model-based iterative reconstruction. *Eur Radiol* 28:2464–2473